



A Systematic Study of Coupling Effects Concerning the Quasi- Elastic Scatter Calculations for $^{48}\text{Ti} + ^{208}\text{Pb}$ and $^{16}\text{O} + ^{142}\text{Ce}$ Systems

Kadhim H. Marza¹, Farah J. Hamood²

^{1,2} Department of Physics, College of Education for pure Sciences, University of Babylon, Iraq.
EMAIL: pure200.kadhun.hasan@student.uobabylon.edu.iq¹, pure.farah.jabar@uobabylon.edu.iq²

Abstract

This study examined the impact of varying the diffused factor and possible profundity (V_0) on the calculations of the proportion of Quasi-elastic scattering to the 'Rutherford' crossing - section ($\sigma_{\text{qel}}/\sigma_{\text{R}}$) and the Distribution of obstacles D_{qel} , utilizing the Wood-Saxon nuclear potential (WS) for the $^{48}\text{Ti} + ^{208}\text{Pb}$ and $^{16}\text{O} + ^{142}\text{Ce}$ systems. Each system employed three distinct values of the diffuseness parameter. Calculations were conducted for Single-channel "SC" and Coupled-channel "CC" systems to attain optimal concordance between theoretical computations and experimental data for both systems, emphasizing The corresponding speed of colliding nucleus and their inherent properties motion, and assessing their influence on the calculations and surface diffusion. Optimal values were achieved for single-channel (SC) calculations employing an inactive target "T" and projectile "P", as well as for double-channel calculations utilizing an inactive target "T" and an energized projectile "P". The chi-square (χ^2) test was employed to compare the optimal diffusion coefficient results across different simulations. In this study, we established the diffusion coefficient as a standard value of 0.63 fm and examined values both above and below this standard. We established a radius of 1.2 fm and the ideal possible profundity (V_0) for both systems, noting variances in the diffusion coefficients. The results indicated that both systems demonstrated concordance between theoretical calculations and experimental data.

Keywords: Quasi-elastic Scatter, Woods-saxon, Possible, Single-channel, Coupled-channels, Diffused factor, Heavy-Ion systems.

Introduction

Quasi-elastic scattering is characterized by the aggregate effects of Elastic Scatter, inelastic Scatter, and transfer reactions. It is deemed analogous toward the fusion reaction, that denotes a process in wherein 2 distinct nuclei amalgamate to form a composite systems[1]. Fusion and Quasi-elastic Scatter are both seen as comprehensive processes and are mutually complementary. Thus, these interactions are regulated by the identical possible and yield equivalent data regarding the interaction systematic. Furthermore, all are susceptible to Channel Coupling effects resulting from collective inelastic excitations of the interaction nuclei at energies close to the Coulomb limit [2]. The Woods-Saxon "WS" form is often utilized to depict the nuclear potential, characterized by profundity parameter " V_0 ", the radius factor " r_0 ", and the diffused factor " a_0 ". This model is crucial in nuclear physics, as it is considered a realistic possibility [3]. Heavy-ion fusion processes are physically analogous to heavy-ion Quasi-elastic Scatter at retrograde angles. At energy levels close to the Coulomb limit, these intricate processes are influenced by Channel Coupling effects arising from the cooperative inelastic excitations of the interacting nuclei. the reflection probability at the Coulomb limit pertains to Quasi-elastic scatter, while crossing past the barrier relates to the fusion process. The interaction concerning the relative velocity of colliding nuclei and their internal degrees of autonomy significantly enhances fusion cross- sections at sub-threshold energy [4]. This study seeks to examine Quasi-elastic Scatter at energies proximate to the Coulomb limit to ascertain the surface diffused factors of the inactive -nuclear possible for the ($^{48}\text{Ti} + ^{208}\text{Pb}$ and $^{16}\text{O} + ^{142}\text{Ce}$) systems. Calculations for single-channel and coupled-channels were conducted with the CQEL code [5], which incorporates all classifications of coupling and embodies the latest version of the "CCFULL" computational framework. The chi- square (χ^2) minimization method was utilised to ascertain the appropriate diffuseness parameters that yield the best alignment with the experimental results. Farah J. Hamood has conducted investigations on Quasi-elastic Scatter in several high- energy ion systems [6 -7].

Theoretical Framework

The nucleus- nucleus possible comprises 2 components: the nuclear component V_N , that can be accurately and reasonably represented by the Woods-Saxon "WS" form, characterized by the conventional volume representation of the true nuclear potential [8]:

$$V_N(r) = \frac{-V_0}{1 + e^{(r-R_0)/a_0}} \quad , \quad (1)$$

The radii of these possibilities. correspond to the possible profundity, with "a" representing the surface diffused factor, "r" denoting the radius factor and number of mass of the target and projectile specified accordingly [9].

$$R_0 = r_0(\sqrt[3]{A_P} + \sqrt[3]{A_T}) \quad , \quad (2)$$

Here, R_0 indicates the radius of the system, while V_0 , a , and r_0 signify the possible profundity, surface diffused factor, and radius factor, in that order. Additionally, r represents the distance of the center of mass between the target "T" nucleus with mass number " A_T " and the projectile "P" nucleus with mass number " A_P ".

The possible between the projectile "P" and the target "T" is defined is a function of the relative distance r between the "centers of mass" of the colliding nuclei. It comprises two components delineated by [10]:

$$V_{\text{eff}}(r) = V_N(r) + V_C(r) \quad (3)$$

The 'Schrödinger equation' for the complete wave function is expressed as [11]:

$$\left(-\frac{\hbar^2}{2\mu} \nabla^2 + V_{\text{eff}}(r) + H_0(\xi) + V_{\text{coup}}(\xi) \right) \psi(\vec{r}, \xi) = E\psi(\vec{r}, \xi) \quad , \quad (4)$$

In this context, r denotes the distance to the "center of mass" between the colliding nuclei, μ signifies the decreased mass of the system, and V_r represents the bare possible in the absence of coupling. The effective potential is expressed as $V_{\text{eff}}(r) = V_N(r) + V_C(r)$. $H_0(\xi)$ indicates the "Hamiltonian" for intrinsic dynamics, while $V_{\text{coup}}(\xi)$ refers to the aforementioned Coupling. The total wave function, $\psi(r \vec{r}, \xi)$, is determined by $r \vec{r}$ and ξ , where ξ represents an internal degree of autonomy. The Quasi-elastic differential cross section can be expressed using the equation [12]:

$$\frac{d\sigma_{\text{qel}}}{d\sigma_R}(E, \theta) = \sum_{j \neq l} \frac{k_{nl}}{k} \left| \frac{f_{j \neq l}(E, \theta)}{f_C(E, \theta)} \right|^2 \quad , \quad (5)$$

where $f_C(E, \theta)$ denotes the Coulomb scattering amplitude and $f_{j \neq l}(E, \theta)$ represents the Quasi-elastic scatter amplitude.

Findings And Discussion

calculations were conducted using the latest version of the CQEL code [5], which represents the latest version of the CCFULL computational framework. This code provides rigorous numerical solutions for the coupled-channel equations and the Schrödinger equation. To minimize systematic errors, a Chi-square (χ^2) optimization technique was employed, wherein data points satisfying $\frac{d\text{qel}}{dR} > 1$ were excluded derived from the fitting protocols. The χ^2 method served as the normalization criterion between theoretical predictions and experimental measurements. The primary potential utilized in this study is the Woods-Saxon (WS) potential, comprising both real and imaginary components; the latter accounts for the relatively weak internal absorption. The parameters of the real potential were specified. methodically modified to attain the optimal alignment with experimental results, a procedure consistently applied across all investigated interactions. A constant value of 0.63fm is adopted for the diffuseness parameter [13], This value is subject to adjustment, either increased or decreased, to account for the specificities of each nuclear system. Furthermore, the radius factor is presumed to be $r_0 = 1.2\text{fm}$.

4.1. The $^{48}\text{Ti} + ^{208}\text{Pb}$ reaction

In the outcomes of this system were analyzed under 2 scenarios: the first scenario involved treating both the projectile "P" and target "T" nuclei as inactive "SC" at varying diffusion parameter values of 0.59, 0.63, and 0.65 fm, with 0.63 fm designated as the normative value. In the second scenario, the ^{48}Ti projectile "P" core was inert, exhibiting a distortion parameter of $\beta_2 = 0.269$ [14] and $\beta_4 = 0.000$ [14] for the 2^+ state (0.983531 MeV), derived from the ratio $E_4^+/E_2^+ = 2.3$. Conversely, the target core ^{208}Pb displayed vibrational characteristics with a distortion factor of $\beta_2 = 0.111$ [14] for the 2^+ state (4.08552 MeV), where $E_4^+/E_2^+ = 1.058$ in the Coupled-channels "CC" framework. We employed the one phonon state of the quadruple excitation of the projectile "P" and target "T" nuclei, with a possible profundity $V_0 = 70$ MeV and a radius parameter $r_0 = 1.2$ fm.

Table1: Present the values of the "WS" possible factors and the χ^2 alignment between empirical and theoretical data for the $^{48}\text{Ti} + ^{208}\text{Pb}$ system.

System	Channel	V_0 (MeV)	r_0 (fm)	a_0 (fm)	$\theta_{c.m}$ (deg)	χ^2	
						$\sigma_{\text{qel}}/\sigma_R$	D_{qel}
$^{48}\text{Ti} + ^{208}\text{Pb}$	SC	70	1.2	0.59	170	0.0164715	0.0318619
				0.63		0.0304536	0.0213461
				0.65		0.0425337	0.0181219
	CC	70	1.2	0.59	170	0.0059971	0.0216779
				0.63		0.0188642	0.0161469
				0.65		0.0304802	0.0150753

Table (1) shows the "Woods-Saxon" nuclear possible parameter employed in the computations for the $^{48}\text{Ti} + ^{208}\text{Pb}$ system, including the possible profundity " V_0 ", the radius coefficient " r_0 ", the surface diffusion parameter a_0 , and the scatter angle " $\theta_{c.m}$ ". The table also includes the chi-square values χ^2 obtained by comparing the theoretical results with the empirical data for both the Quasi-elastic scattering Cross-section ratio ($\sigma_{\text{qel}}/\sigma_R$) and the distribution of obstacles D_{qel} . The outcomes show that the lowest chi-square value in the single-channel (SC) calculations was obtained at 0.59 fm. The χ^2 is 0.0164715, indicating that this value provides the best concordance with the experimental

data in comparison to the others values. In the case of coupled channels (CC), the χ^2 values decreased significantly, reaching 0.0059971 at the same value for the diffusion parameter, indicating that incorporating the coupling effects between different channels leads to a clear improvement in depicting the Quasi-elastic scatter data. Overall, the results show that the Quasi-elastic scatter calculations are highly sensitive to the value of the surface diffusion parameter and that smaller values for the diffusion parameter provide better agreement with the experimental measurements in the system under study. The optimal value of barrier distribution was $a_s = 0.65$, and the χ^2 was 0.0181219 in both Single-Channel and Conjugate-channels. These results represent the best concordance with the experimental data.

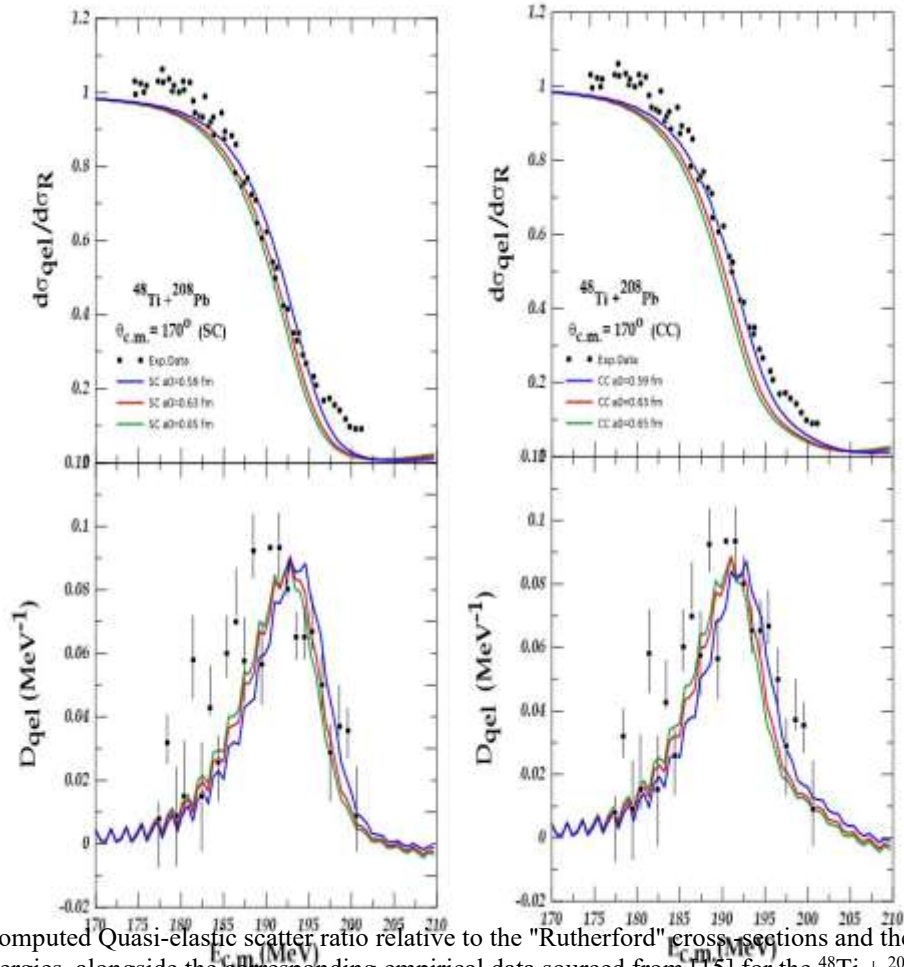


Figure 1: The computed Quasi-elastic scatter ratio relative to the "Rutherford" cross sections and the distribution at sub-barrier energies, alongside the corresponding empirical data sourced from [15] for the $^{48}\text{Ti} + ^{208}\text{Pb}$ system, is presented for Single-channel "SC" and Coupled-channels "CC" calculations at $a_s = (0.59, 0.63, \text{ and } 0.65 \text{ fm})$, denoted in blue, red, and green, respectively.

Figure (1) illustrates the ratio of the Quasi-elastic scattering cross-section to the "Rutherford" scattering ($\sigma_{\text{qel}}/\sigma_{\text{R}}$) as a function of the center-of-mass energy $E_{\text{c.m.}}$, alongside the distribution of obstacles D_{qel} for the $^{48}\text{Ti} + ^{208}\text{Pb}$ system at an angle of 170° . Experimental data are depicted as black dots, whereas the colored curves illustrate the computed theoretical outcomes for three distinct values of the surface diffusion parameter. The outcomes of the single-channel (SC) computations are presented, with the blue curve indicating the calculation at $a_s = 0.59 \text{ fm}$, the red curve representing the calculation at $a_s = 0.63 \text{ fm}$, and the green curve denoting the calculation at $a_s = 0.65 \text{ fm}$. The blue curve demonstrates superior concordance with the empirical data, particularly in the energy vicinity of the Coulomb obstacle, suggesting that the reduced diffusion coefficient yields a more precise characterization of the nuclear possible profile at the nuclear surface. The results of the coupled-channel (CC) calculations for identical diffusion parameter values are presented, indicating a significant enhancement in the concordance between theoretical calculations and experimental data. The optimal value was seen at $a_s = 0.65 \text{ fm}$, represented by the green curve. The introduction of coupling effects alters the effective barrier of the reaction by partitioning it into multiple sub-barriers linked to the aggregate excitations of the reacting nuclei, while the distribution of obstacles, D_{qel} , is derived from the derivative of the Quasi-elastic cross-Section ratio concerning energy. The distribution displays a distinct peak that aligns with the system's effective interaction barrier. The optimal value for the distribution at a diffused factors of 0.65 is denoted by the green curve, which signifies the most favorable alignment with the experimental data.

Table 2.: The parameters of the "WS" possible factors and the χ^2 alignment between empirical and theoretical data for the $^{48}\text{Ti} + ^{208}\text{Pb}$ system.

System	Channel	a_s (fm)	r_o (fm)	V_o (MeV)	$\theta_{c.m}$ (deg)	χ^2	
						σ_{qel}/σ_R	D_{qel}
$^{48}\text{Ti} + ^{208}\text{pb}$	SC	0.59	1.2	65	170	0.0117108	0.0355237
				70		0.0164715	0.0318619
				79		0.0367076	0.0273256
	CC	0.59	1.2	65	170	0.0038212	0.0239544
				70		0.0059971	0.0216779
				79		0.0158869	0.0192863

Table (2) shows the "Woods-Saxon" possible parameters utilized in the present calculations for the $^{48}\text{Ti} + ^{208}\text{Pb}$ system at the scattering angle $\theta_{c.m}$. The angle is 170° , with a fixed radius parameter r_o of 1.2 fm and a surface diffuseness a_s of 0.59 fm. The table additionally displays the associated chi-square values (χ^2) derived from the comparison of theoretical calculations with empirical data for both the Quasi-elastic cross-Section ratio (σ_{qel}/σ_R) and the distribution of obstacles D_{qel} . For the single-channel (SC) calculations, the smallest chi-square value for the cross-section ratio is obtained at $V_o=65$ MeV with $\chi^2 = 0.0117108$, indicating that this potential depth provides the best agreement with the experimental data within the SC framework. As the potential depth increases to 70 and 79 MeV, the chi-square values increase, reflecting a gradual deterioration in the agreement with the experimental measurements. A similar trend is observed for the barrier distribution D_{qel} , where the lowest chi-square value also corresponds to $V_o=65$ MeV. This outcome validates the significant sensitivity of the obstacle distribution to the selection of nuclear potential parameters. Regarding the coupled-channels (CC) computations, the chi-square values are significantly reduced compared with the single-channel (SC) results, demonstrating the significance of coupling effects in describing the quasi-elastic scattering process. The minimum chi-square value for the cross-section ratio is obtained at 65 MeV with $\chi^2=0.0038212$, which represents the best overall concordance with the empirical facts.

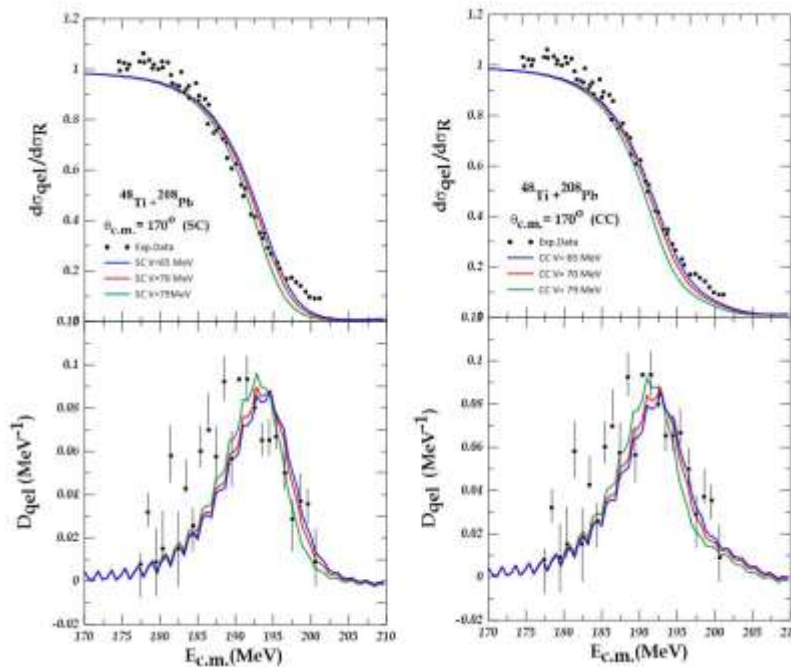


Figure 2 illustrates the Quasi-elastic scatter ratio relative to the "Rutherford" cross-Section and the barrier distribution at sub-barrier energies, accompanied by the corresponding empirical data from Single-channel "SC" and Coupled-channel "CC" computations for $V = (65, 70, \text{ and } 79 \text{ MeV})$. The results are indicated in blue, red, and green, respectively, and the black dots represent experimental data. [15]

Figure (2) shows the ratio of the Quasi-elastic scattering cross section to the Rutherford (σ_{qel}/σ_R) as a function of the center-of-mass energy $E_{c.m}$. The upper part represented Single-channel "SC" and Coupled-channel "CC" calculations, together with the barrier distribution D_{qel} in the lower part for the system $^{48}\text{Ti} + ^{208}\text{Pb}$ at $\theta_{c.m.} = 170^\circ$. The experimental data are depicted by black points, whereas the solid-Colored curves correspond to the theoretical calculations performed for three different potential depths. The blue curve signifies $V_o = 65$ MeV, the red curve corresponds to $V_o = 70$ MeV, and the green curve represents $V_o = 65$ MeV, while the diffusivity factor is kept fixed at $a_s = 0.59$ fm. In

the SC, the theoretical curves show noticeable sensitivity to the variation of the potential depth. The blue curve corresponding to $V_0 = 65$ MeV follows the experimental data more closely in the nearness of the Coulomb limit, whereas increasing the possible depth gradually shifts the theoretical calculations away derived from the empirical data, particularly in the sub-threshold region. The CC calculations at identical potential depths demonstrate a substantial enhancement in the concordance among theoretical calculations and empirical findings, attributable to the incorporation of coupling effects. The Coupled-channels calculations reproduce the slope and magnitude of the experimental data more accurately, indicating the significant role of nuclear structure effects in Quasi-elastic scattering near the Coulomb limit. The barrier distribution in the SC and CC shows the best correspondence at $V_0 = 79$ MeV and denotes that by the green curve.

4.2. The $^{16}\text{O} + ^{142}\text{Ce}$ system

In the outcomes of this system were analysed in two scenarios: the first scenario involved both the projectile "P" and target "T" nuclei being treated as inactive "SC" at varying diffusion parameter values of 0.60, 0.63, and 0.66 fm, with 0.63 fm designated as the normative value. In the second scenario, the nucleus of the ^{16}O projectile "P" was in a vibrational state, defined by a deformation parameter of $\beta_2 = 0.729$ [12] for the 2^+ state (6.9171 MeV); this was inferred from the ratio $E_4^+/E_2^+ = 1.497$. In contrast, the nucleus of the ^{142}Ce target was similarly in a vibrational state, although it is regarded as inert due to the deformation parameter $\beta_2 = 0.000$ [12] for the 2^+ state (0.64128 MeV), where the ratio $E_4^+/E_2^+ = 1.9014$ equated to 1.058 under the Coupled Channels (CC) model. A single-phonon state for quadrupole excitation was utilised for both the projectile "P" and target "T" nuclei, employing a possible profundity of $V_0 = 30$ MeV and a radius factor of $r_0 = 1.2$ fm.

Table 3: Display the values of the "WS" possible factors and the χ^2 alignment between empirical and theoretical data for the $^{16}\text{O} + ^{142}\text{Ce}$ system.

System	Channel	V_0 (MeV)	r_0 (fm)	a_0 (fm)	$\theta_{c.m.}$ (deg)	χ^2	
						σ_{qel}/σ_R	D_{qel}
$^{16}\text{O} + ^{142}\text{Ce}$	SC	30	1.2	0.60	180	0.1419183	0.5026162
				0.63		0.1868446	0.3885636
				0.66		0.2312862	0.3054423
	CC	30	1.2	0.60	180	0.1038389	9.5377480
				0.63		0.1361290	0.6069134
				0.66		0.1704163	0.1936776

Table 3: shows the Woods-saxon nuclear possible parameters utilized in the computations for the $^{16}\text{O} + ^{142}\text{Ce}$ system, including the possible profundity " V_0 ", radius coefficient " r_0 ", the exterior diffusion coefficient a_0 , and the scattering angle. The table also includes the chi-square values χ^2 obtained by comparing the theoretical results with the empirical data for both the Quasi-elastic scattering Cross-section ratio (σ_{qel}/σ_R) the distribution of obstacles D_{qel} . The outcomes show that the lowest chi-square value in the single-channel (SC) calculations was obtained at $a_0 = 0.60$ fm, which is 0.1419183, indicating that this value provides the best accord with the experimental data in comparison to the others values. In the case of coupled channels (CC), the χ^2 values decreased significantly, reaching 0.1038389 at the same value for the diffusion parameter, indicating that incorporating the coupling effects between different channels leads to a clear improvement in describing the Quasi-elastic scatter data. The optimal value of the distribution of obstacles D_{qel} measures 0.3054423 in the single channel, while in the coupled channel it is 0.1936776 at the same value of $a_0 = 0.66$ fm. Consequently, the diffusivity factor derived from a Coupled-channels calculation should be prioritized over that acquired from a single channel calculation, as anticipated.

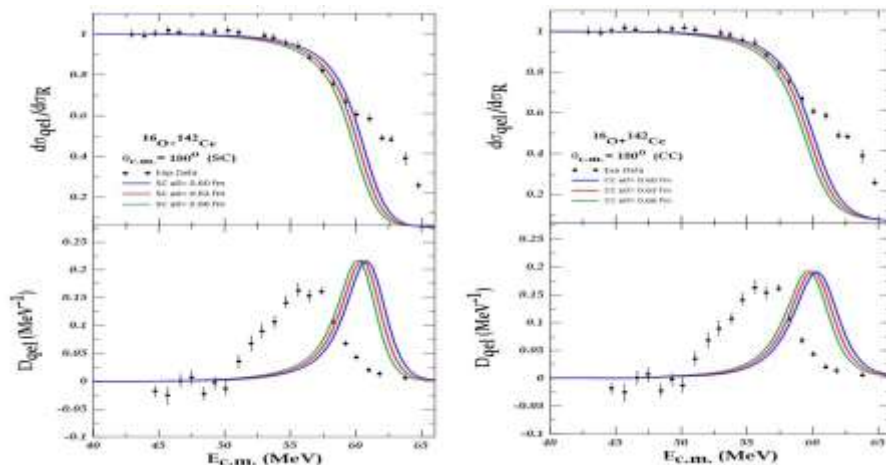


Figure 3 The calculated Quasi-elastic scatter ratio to the "Rutherford" Cross-sections and the distribution at the Sub-barrier energies with the corresponding empirical data taken from [16] for the system $^{16}\text{O} + ^{142}\text{Ce}$ in the Single-channel "SC" and Coupled-channels "CC" calculations at $a_s = (0.60, 0.63, \text{ and } 0.66 \text{ fm})$, indicated as blue, red, and green, respectively.

Figure 3 illustrates the ratio of the Quasi-elastic scattering cross-section to the "Rutherford" scattering ($\sigma_{\text{qel}}/\sigma_{\text{R}}$) as a function of the center-of-mass energy $E_{\text{c.m.}}$, alongside the barrier distribution D_{qel} for the $^{16}\text{O} + ^{142}\text{Ce}$ system at an angle of 180 degrees. Experimental data are represented by black dots, while the colored curves represent the calculated theoretical results for three distinct values of the surface diffusion coefficient. The results of the single-channel "SC" calculations are shown, where the blue curve signifies the computation at $a_s = 0.60 \text{ fm}$, the red curve the calculation at $a_s = 0.63 \text{ fm}$, and the green curve the calculation at $a_s = 0.66 \text{ fm}$. The blue curve shows better agreement with the experimental data, particularly at the energy vicinity of the Coulomb limit. The findings of the Coupled-channel "CC" calculations, utilising a vibrating projectile "P" and an inactive target "T" with identical diffusion coefficient values, demonstrate a significant enhancement in the concordance between experimental data and theoretical simulations. The optimal value occurs at a diffuseness coefficient of 0.60 fm, illustrated by the blue curve. This is attributable to coupling effects alter the reaction's effective barrier by dividing it into many sub-barriers connected to the aggregate excitations of the reacting nuclei. The barrier distribution D_{qel} is derived from the derivative of the Quasi-elastic Cross-section ratio about energy. The distribution exhibits a well-defined peak corresponding to the effective interaction barrier of the system. The optimal value of the distribution at 0.66 fm is indicated by the green curve, which represents the best overall agreement with experimental facts.

Table 4: Displays the parameters of the "WS" possible factors and the χ^2 alignment between empirical and theoretical data for the $^{16}\text{O} + ^{142}\text{Ce}$ system.

System	Channel	a_s (fm)	r_0 (fm)	V_0 (MeV)	$\theta_{\text{c.m}}$ (deg)	χ^2	
						$\sigma_{\text{qel}}/\sigma_{\text{R}}$	D_{qel}
$^{16}\text{O} + ^{142}\text{Ce}$	SC	0.60	1.2	26	180	0.0531022	0.5604890
				30		0.1360041	0.4710989
				33		0.2586446	0.4173495
	CC	0.60	1.2	26	180	0.0814802	1.1465040
				30		0.1754794	11.6646700
				33		0.2929162	0.2240452

Table (4) lists the "Woods-saxon" possible parameters utilized in the present calculations for the $^{16}\text{O} + ^{142}\text{Ce}$ system at the scattering angle of 180° , with a fixed radius parameter r_0 of 1.2 fm and a surface diffuseness a_s of 0.60 fm. The table also presents the corresponding chi-square values (χ^2) obtained from the comparison between the theoretical computations and the empirical facts for both the Quasi-elastic Cross-section ratio ($\sigma_{\text{qel}}/\sigma_{\text{R}}$) and the distribution of obstacles D_{qel} . For the single-channel (SC) calculations, the smallest chi-square value for the cross-section ratio is obtained at $V_0=26 \text{ MeV}$ with $\chi^2=0.0531022$, indicating that this potential depth provides the best agreement with the experimental data within the SC framework. As the potential depth increases to 30 and 33 MeV, the chi-square values increase, reflecting a gradual deterioration in the agreement with the experimental measurements. A similar trend is observed for the barrier distribution D_{qel} . This result confirms the strong sensitivity of the obstacle distribution to the choice of the nuclear capability parameters. In the case of the Coupled-channels "CC" calculations, the chi-square values are significantly reduced compared with the single-channel (SC) results, demonstrating the significance of coupling effects in describing the quasi-elastic scattering process. The minimum chi-square value for the cross-section ratio is obtained at 26 MeV with $\chi^2=0.0814802$, which represents the best overall contract with the empirical data. Comparing the current results with the previous computations, where the diffuseness parameter was varied while keeping the potential depth fixed, it can be concluded that the surface diffuseness mainly governs the configuration of the barrier dispersion. Therefore, an appropriate combination of both parameters is essential for achieving an accurate description of the reaction dynamics in heavy-ion quasi-elastic scattering.

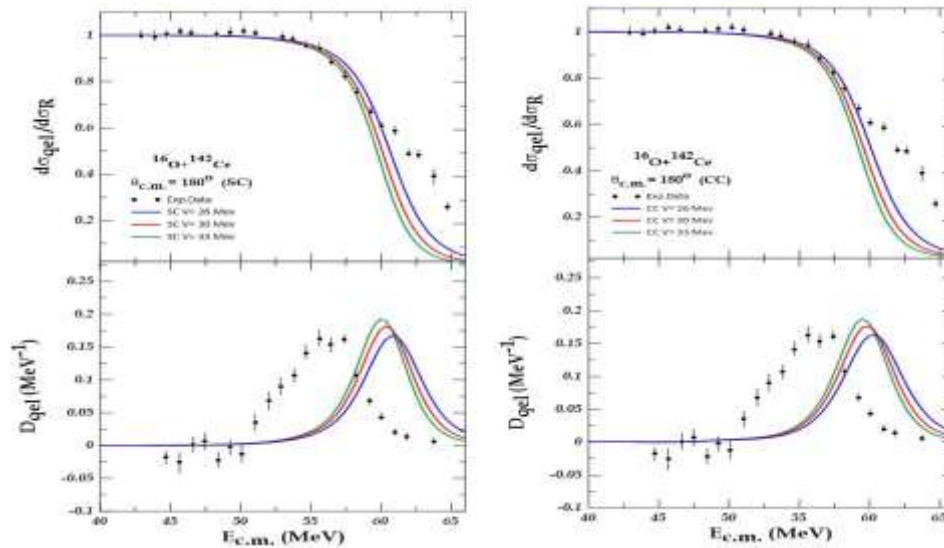


Figure (4): The Quasi-elastic scatter ratio relative to the "Rutherford" Cross-sections and the distribution at sub-barrier energies are juxtaposed with the equivalent empirical data from Single-channel "SC" and Coupled-channel "CC" simulations for $V_0 = 26, 30,$ and 33 MeV. Red, green, and black denote the outcomes, whereas the black dots signify experimental data. [16]

Figure (4) shows the ratio of the Quasi-elastic scattering cross section to the "Rutherford" (σ_{qel}/σ_R) as a function of the center-of-mass energy $E_{c.m.}$ together utilising the barrier distribution D_{qel} for the system $^{16}\text{O} + ^{142}\text{Ce}$ at $\theta_{c.m.} = 180^\circ$. The empirical data is represented by black points, whereas the solid-colored curves correspond to the theoretical calculations performed for three different potential depths. The blue curve denotes $V_0 = 26$ MeV, the red curve signifies $V_0 = 30$ MeV, and the green curve indicates $V_0 = 33$ MeV, while the diffuseness parameter is kept fixed at $a_0 = 0.60$ fm. The top two parts of the figure show the results of the Single-channel "SC" and Coupled-channel "CC" calculations, where the "SC" calculations show the theoretical curves are remarkably sensitive to changes in voltage depth. The curve corresponding to $V_0 = 26$ MeV follows the experimental data more closely in the nearness of the Coulomb barrier, whereas increasing the potential depth gradually shifts the theoretical calculations away from the empirical data, particularly within the sub-barrier domain. While in the results of the coupled channel, the accord between the theoretical results and the empirical data is clearly improved due to the inclusion of coupling effects. In the experiment involving a vibrating projectile "P" and an inert target "T", the optimal value was determined at the potential profoundness $V_0 = 26$ MeV, as illustrated by the blue curve. The optimal value for the allocation at a potential depth of 33 MeV is represented by the green curve, which represents the best overall agreement with the experimental data.

Conclusions

This investigation leads us to the following conclusions:

- 1- The factor of surface diffuseness a_0 significantly influences the characteristics of Quasi-elastic scatter and the configuration of the distribution of obstacles for both systems ($^{48}\text{Ti} + ^{208}\text{Pb}$ and $^{16}\text{O} + ^{142}\text{Ce}$). Variations in a_0 produce more pronounced changes in the calculated observables. The results of χ^2 clearly demonstrated this behavior.
- 2- The inclusion of coupled-channels (CC) effects leads to a significant improvement in the agreement between theoretical computations and empirical facts for all examined scenarios. The CC calculations consistently yield lower (χ^2) values and smoother, more realistic distributions, highlighting the essential role of channel coupling in describing heavy-ion interactions.

Reference

1. Hagino K, Takehi T, Balantekin AB, Takigawa N. Surface diffuseness anomaly in heavy-ion potentials for large-angle quasielastic scattering. *Physical Review C* 2005; 71(4): 44612.
2. Andres MV, Rowley N, Nagarajan MA. Effect of deformation on the elastic and quasielastic scattering of heavy ions near the Coulomb barrier. *Physics Letters B* 1988; 202(3): 292–295.
3. L.R. Gasques, M. Evers, D.J. Hinde, M. Dasgupta, P.R.S. Gomes, R.M. Anjos, M.L. Brown, et al., "Systematic study of the nuclear potential through high precision back-angle quasi-elastic scattering measurements," *Phys. Rev. C - Nucl. Phys.* 76(2), 024612 (2007).
4. M. Dasgupta, D.J. Hinde, N. Rowley, and A. M. Stefanini, "Measuring Barriers To Fusion," *Annual Review of Nuclear and Particle Science*, 48, 401-461 (1998).
5. K. Hagino, N. Rowley, and A.T. Kruppa, "A program for coupled-channel calculations with all order couplings for heavy-ion fusion reactions," *Comput. Phys. Commun.* 123(1-3), 143-152 (1999).

6. Farah J. Hamood§, Khalid S. Jassim The Effect Of Diffuseness Parameter On The Quasi-Elastic Scattering Of The $^{25}\text{Mg} + ^{90}\text{Zr}$ And $^{28}\text{Si} + (^{120}\text{Sn}, ^{150}\text{Nd})$ Systems Using Wood-Saxon Potential .April 30; 282-288 (2023)
7. Farah J. Hamood, Khalid S. Jassim The Influence Changing of Nuclear Potential On Quasi-Elastic Scattering In $^{16}\text{O} + ^{160}\text{Gd}$ And $^{12}\text{C} + ^{197}\text{Au}$ Systems. 305-310 ,ISSN 2312-4334(2023)
8. Rehm KE. Quasi-elastic heavy-ion collisions. Annual Review of Nuclear and Particle Science 1991; 41(1): 429–468.
9. Wang N, Liu M, Yang Y. Heavy-ion fusion and scattering with Skyrme energy density functional. Science China Physics, Mechanics & Astronomy 2009; 52(10): 1554–1573.
10. Timmers H, Leigh JR, Dasgupta M, Hinde J, Lemmon RC, Mein JC, Rowley N. Probing fusion barrier distributions with quasi-elastic scattering. Nuclear Physics A 1995; 584(1): 190–204.
11. Piasecki E, Kowalczyk M, Piasecki K, Srebrny J, Witecki M, Carstoiu F, Kisieliński M. Barrier distributions in $^{16}\text{O} + ^{116,119}\text{Sn}$ quasielastic scattering. Physical Review C 2002; 65(5): 54611.
12. Zagrebaev VI. Understanding the barrier distribution function derived from backward-angle quasi-elastic scattering. Physical Review C 2008; 78(4): 47602.
13. M. Dasgupta, D.J. Hinde, J.O. Newton, and K. Hagino, “The nuclear potential in heavy-ion fusion,” Prog. Theor. Phys. Suppl. 154, 209-216 (2004).
14. S. Raman, C. W. Nestor Jr, and P. Tikkanen, "Transition probability from the ground to the first-excited 2^+ state of even even nuclides," At. Data Nucl. Data Tables, vol. 78, no. 1, pp. 1 128, 2001.
15. Wen PW, Chuluunbaatar O, Descouvemont P, Gusev AA, Lin CJ, Vinitzky SI. Role of multi-phonon and high-spin states on the quasi-elastic barrier distributions of massive systems. Physics Letters B 2025; 863: 139383.
16. Biswas R, Nath S, Gehlot J, Gonika, Kumar C, Parihari A, Madhavan N, Vinayak A, Mahato A, Noor S, Sherpa P. Fusion barrier distribution from measurement of quasielastic scattering at $\theta_{c.m.}=180^\circ$. Journal of Physics: Conference Series 2023; 2586: 012050.